

Reinforcement Learning based Beamforming for Massive MIMO Radar Multi-target Detection

Aya Mostafa Ahmed, *Student Member, IEEE*, Alaa Alameer Ahmad, *Student Member, IEEE*, Stefano Fortunati, *Member, IEEE*, Aydin Sezgin, *Senior Member, IEEE*, Maria S. Greco, *Fellow, IEEE*, Fulvio Gini, *Fellow, IEEE*

Abstract—This paper considers the problem of multi-target detection for massive multiple input multiple output (MMIMO) cognitive radar (CR). The concept of CR is based on the perception-action cycle that senses and intelligently adapts to the dynamic environment in order to optimally satisfy a specific mission. However, this usually requires a priori knowledge of the environmental model, which is not available in most cases. We propose a reinforcement learning (RL) based algorithm for cognitive beamforming in the presence of unknown disturbance statistics. The radar acts as an agent which continuously senses the unknown environment (i.e., targets and disturbance). Consequently, it optimizes the beamformers through tailoring the beampattern based on the acquired information. Furthermore, we propose a solution to the beamforming optimization problem with less complexity than the existing methods. Numerical simulations are performed to assess the performance of the proposed RL-based algorithm in both stationary and dynamic environments. The RL based beamforming is compared to the conventional omnidirectional approach with equal power allocation. As highlighted by the proposed numerical results, our RL-based beamformer greatly outperforms the omnidirectional one in terms of target detection performance. The performance improvement is even more remarkable under environmentally harsh conditions such as low SNR, heavy-tailed disturbance and rapidly changing scenarios.

Index Terms—Cognitive Radar, Reinforcement learning, Massive MIMO, unknown disturbance distribution, Beamforming.

I. INTRODUCTION

Cognitive radar (CR) paradigm has been firstly introduced by Haykin taking inspiration from echo-location of some mammals like bats or dolphin [1], and cognition in human brains [2]. CR is described as a radar system which senses the environment, learns from it and makes decisions based on what it has learned to accomplish certain assigned tasks through a perception-action cycle of cognition. As a matter of fact, this cycle starts with the illumination of the environment by transmitting a waveform, then from the reflected radar

Funded by the Deutsche Forschungsgemeinschaft (DFG, German Research Foundation) Project-ID 287022738 TRR 196 (S03)

A. M. Ahmed, A. A. Ahmad, and A. Sezgin are with the Institute of Digital Communication Systems, Ruhr University Bochum, 44801 Bochum, Germany (e-mail: aya.mostafaibrahimahmad@rub.de; alaa.alameerahmad@rub.de; aydin.sezgin@rub.de).

S. Fortunati, is with Università di Pisa, Dipartimento di Ingegneria dell'Informazione, Pisa, Italy and with Université Paris-Saclay, CNRS, CentraleSupélec, Laboratoire des signaux et systèmes, 91190, Gif-sur-Yvette, France. (e-mail: stefano.fortunati@centralesupelec.fr).

M. S. Greco, and F. Gini is with Università di Pisa, Dipartimento di Ingegneria dell'Informazione, Via Caruso, 56122, Pisa, Italy. (e-mail:m.greco@iet.unipi.it; f.gini@ing.unipi.it).

echos, it learns the dominant information about the target and the surroundings (perception). Finally it adapts the optimal transmit waveform accordingly to accomplish a desired goal (action) [1]. In a non-stationary environment, this cycle is repeated continuously, where the non-stationarity can be caused by statistical weather variations, stochastic disturbance or the presence of unknown non-static targets. Whereas, the disturbance in radar is produced by two components, the clutter and white Gaussian noise. In [2], Haykin clearly distinguishes between traditional feed forward radar, fully adaptive radar, and a CR. A radar is considered adaptive, when it employs a global feedback including the environment in this feedback loop, where adaptive filtering at the receiver or adaptive beamforming at the transmitter might be applied [3]. However, CR develops its own behavior rules from the experience gained, stores it in the memory, and extends this knowledge to the transmitter. This is followed by a set of smart decision-actions. Hence, it can be deduced that CRs would benefit significantly from the waveform diversity at the transmitter offered by multiple input multiple output (MIMO) radar systems. Unlike phased arrays, MIMO takes advantages of transmitting multiple correlated or uncorrelated probing signals, offering higher degrees of freedom (DoF). There are two main types of MIMO radar systems: *widely separated* and *colocated*. A widely separated MIMO radar exploits the spatial diversity of the target's radar cross section (RCS) by using widely separated transmit/receive antennas [4]. On the other hand, the antenna of a colocated MIMO radar are closely spaced, allowing for significant coherent gain when combining the probing signals, which can be achieved through designing the transmit beampattern [5]. This latter type is quite appealing for CR systems, since the transmitter can optimize the beampattern based on the received radar echoes. Furthermore, the transmit beampattern can be shaped to suppress disturbance in some directions and maximize the gains in the desired ones [6].

While the advantages of MIMO radar have been extensively discussed in the literature, in terms of spatial resolution [7], parameter identifiability [8] and interference rejection capabilities [9], there are only a few works unveiling the potential benefits of large scale MIMO radars. Recently, massive multiple input multiple output (MMIMO) has transformed from just an idea [10] to reality, where commercial solutions with up to 64 fully digital transceivers are adopted for 5G [11]. Moreover, as foreseen in [12], with the higher DoFs offered by MMIMO, new areas can be explored. For instance, in the detection of

small unmanned vehicles (UAV) whose RCS can be up to three orders of magnitude smaller than manned vehicles. In such a case, the probability of detection P_D of these UAVs can be below 0.5 for constant false alarm of $P_{FA} = 10^{-5}$ [13]. However, there are key questions that are still not discussed in the literature. One of the main open problems of MMIMO radar is the design of robust algorithms for detection and estimation with scalable complexity as the number of deployed antennas increases. Moreover, cognitive MMIMO radar, requires optimizable waveforms [14]. Hence, the design of scalable and fast accurate optimization algorithms is necessary. Complementary and equally essential as the waveform diversity at the transmitter, is the receiver cognition, which guides the radar decisions and controls the choice of the waveforms. In [1], [2], [15], the authors utilized Bayesian filtering for the perception-action cycle, where the receiver makes probabilistic predictions on the next environmental state given the current state. However, it is prone to model mismatches as it depends on prior information of the environment dynamics. To avoid this dependence, reinforcement learning (RL) is adopted for cognitive radars in [16], [17]. RL is an area of machine learning which maps scenarios to actions in order to maximize a certain reward function [18]. RL can address model free problems by using software defined agents, which learn from the observations captured from the environment, and take the best possible actions. Specifically, the agent calculates rewards through exploration of the environment, and produces control policies to attain a certain goal. The outcomes usually are unclear at first, then this agent learns by experience. In this paper, we propose to use RL for multi-target detection for a MMIMO CR system. The agent in our setup is the radar, and the environment contains targets and disturbance. We assume no prior information about the environment, where the number of targets, and disturbance statistics are unknown. Our algorithm can be summarized as follows

- 1) transmit orthonormal waveforms corresponding to omnidirectional beam,
- 2) the radar agent collects information about the environment (targets and disturbance) from the received echoes,
- 3) this information is used to calculate the reward,
- 4) the beamformers are optimized to shape the beampattern towards the most probable target locations.

A. Related Work

The use of machine learning with CR has been recently explored in the literature. In [16], [17] RL-CR is used for dynamic spectrum allocation, while in [19] the authors use CR for target detection in an end-to-end learning approach. They propose an alternating procedure to jointly design the transmit waveform and the detector. A neural network is used to approximate the generalized likelihood ratio test (GLRT) while the transmit waveform is fixed. Afterwards, for a fixed detector, they train the transmitted waveform using deep RL. However, there is no statistical guarantee on the resulting P_D and P_{FA} in the presence of different disturbance models than the ones used in training. Hence, the performance is sensitive to deviations of the considered model. Moreover, they

don't address multi-target detection. In [20], the authors use machine learning approaches to estimate the optimal detection threshold, based on non-linear transformation of the order statistics. Yet, they use an offline library for the disturbance distributions, where they assume a priori known covariance matrix to build this library. In contrast, our algorithm uses only the data collected from the current environment without the need of any offline knowledge of possible disturbance distributions nor their covariance matrix. In [21], RL has been used in indoor mapping for UAV applications. Mechanical beamforming using the UAV rotation is used for target detection. However, only Gaussian noise is considered in the detection algorithm. In the context of MMIMO, the work in [22] develops a closed form P_D and P_{FA} expressions using methods from random matrix theory. However, the use of such expressions is not always practical, due to the fact that most of the time, the detector will have insufficient observations to satisfy those assumptions.

B. Contributions

This paper includes several contributions which can be summarized as the following :

- 1) We employ a MMIMO CR detection algorithm based on RL in the presence of disturbance, which is rarely analyzed in the literature. We don't assume any prior information about the distribution of the disturbance, or the number of targets.
- 2) We adopt a RL algorithm to predict the best possible decision rule according to the environment. In fact, we use a novel reward function to predict the next action of the agent. This reward is calculated in terms of a closed-form expression for P_D in asymptotic regimes regardless of the disturbance distribution [23, Corrolary 1]. An asymptotic regime here means when the number of spatial virtual antenna channels N grows unbounded, i.e., $N \rightarrow \infty$. Furthermore, in our case the detector satisfies the constant false alarm rate (CFAR) property using a single snapshot.
- 3) Unlike the works relying on semi-definite programming (SDP) to solve for the beampattern optimization problem [24], [25], we use a beamforming optimization approach that can scale up with a large number of antenna. Moreover, in [24], [25], the beamforming was done in two steps. In the first step, the covariance matrix was optimized. In the second step, this matrix was used to synthesize the beamformers. This imposed further complications to the problem. However, in our algorithm, we optimize directly the beamformers in only one step.
- 4) As suggested by the numerical results, the algorithm is able to detect low SNR targets with a radar operating under $P_{FA} = 10^{-5}$. Moreover, it is robust to environmental changes, e.g., it can detect fading targets and targets changing their angular positions.

II. PROBLEM FORMULATION

We consider a colocated MIMO radar system with N_T transmit antennas and N_R receiver antennas. Both are uniform

linear arrays (ULA) with $\frac{\lambda}{2}$ spacing between the antennas, where λ is the operating wavelength. Let us first assume that one target is present, and the disturbance statistics are unknown.

A. System Model

The complex baseband of the received signal at time t reflected from one point target is defined as [5], [26]

$$\mathbf{y}(t) = \alpha \mathbf{a}_R(\theta) \mathbf{a}_T^T(\theta) \mathbf{s}(t - \tau) + \mathbf{c}(t) \quad (1)$$

where $\mathbf{y}(t) \in \mathbb{C}^{N_R}$. The transmit and receive arrays are characterized by the array manifolds: $\mathbf{a}_T(\theta)$ for the transmitter and $\mathbf{a}_R(\theta)$ for the receiver. θ is the target direction relative to both arrays. Hence, $\mathbf{a}_R(\theta) = [1, e^{j\pi \sin \theta}, \dots, e^{j\pi(N_R-1) \sin \theta}]^T$, and $\mathbf{a}_T(\theta)$ is defined similarly. $\alpha \in \mathbb{C}$ accounts for the radar RCS, and the two way path loss, while τ is the time delay due to the target position with respect to the radar. $\mathbf{c}(t) \in \mathbb{C}^{N_R}$ is the random disturbance vector, which is produced by clutter and white Gaussian noise. $\mathbf{s}(t) \in \mathbb{C}^{N_T}$ is the transmit signal from all N_T antennas, generated as linear combination of independent orthogonal signals $\Phi(t) \in \mathbb{C}^{N_T}$, where

$$\mathbf{s}(t) = \mathbf{W} \Phi(t), \quad (2)$$

and $\mathbf{W} = [\mathbf{w}_1, \dots, \mathbf{w}_{N_T}]^T \in \mathbb{C}^{N_T \times N_T}$, $\mathbf{w}_m \in \mathbb{C}^{N_T}$ describe the beamforming weight matrix. Moreover, \mathbf{W} is a square matrix which must obey the trace constraint $\text{tr}\{\mathbf{W} \mathbf{W}^H\} = P_T$, where P_T is the total transmit power. Furthermore, the beam pattern produced by the transmitted waveforms can be expressed as $B(\theta) = \mathbf{a}_T^T(\theta) \mathbf{R}_W \mathbf{a}_T^*(\theta)$, where $\mathbf{R}_W = \mathbf{W} \mathbf{W}^H$ is the covariance matrix.

Afterwards, the received signal is processed by a linear matched filter $\Phi(t)$ tuned at delay $\hat{\tau}$ considering a single transmitted pulse and one angle cell, such that

$$\mathbf{Y}(\hat{\tau}) = \int_0^T \mathbf{y}(t) \Phi^H(t - \hat{\tau}) dt. \quad (3)$$

Hence,

$$\mathbf{Y} = \alpha \mathbf{a}_R(\theta) \mathbf{a}_T^T(\theta) \mathbf{W} \int_0^T \Phi(t - \tau) \Phi^H(t - \hat{\tau}) dt + \mathbf{C}, \quad (4)$$

where $\mathbf{Y} \in \mathbb{C}^{N_R \times N_T}$, and $\mathbf{C} = \int_0^T \mathbf{c}(t) \Phi^H(t - \hat{\tau}) dt$. We assume that the matched filter is perfectly tuned to the target delay [26], hence $\hat{\tau} = \tau$, and $\int_0^T \Phi(t - \tau) \Phi^H(t - \hat{\tau}) dt = \mathbf{I}$. Rewriting eq. (1) to be in a vector form as

$$\mathbf{y} = \text{vec}(\mathbf{Y}) = \alpha \mathbf{h}(\theta) + \mathbf{c}, \quad (5)$$

where $\text{vec}(\cdot)$ denotes the vectorization operator, such that $\mathbf{y} \in \mathbb{C}^{N_R N_T}$. Moreover $\mathbf{c} = \text{vec}(\mathbf{C})$ denotes the spatially colored disturbance vector. Then, utilizing the properties of the Kronecker product, the vector \mathbf{h} is defined as:

$$\mathbf{h}(\theta) = (\mathbf{W}^T \mathbf{a}_T(\theta)) \otimes \mathbf{a}_R(\theta). \quad (6)$$

B. Disturbance Model

Disturbance represents a critical challenge for detection algorithms, since it can be mistaken as a target triggering a false alarm. However, it is often ignored in a lot of work in the literature [5], [24]–[26] for simplicity, where only temporally and spatially white Gaussian noise is considered. In addition, others assumed the disturbance to have known distributions i.e., K , Pareto, and Weibull distributions as [19], [20], [27]. However, the statistical characterization of disturbance is a difficult task [12], and in reality it is usually unknown. Hence, most of those models are mismatched when compared to true data, and this may highly affect the radar performance [28]. Strong sidelobe disturbance can mask weak targets (i.e., at low SNR), or even lead to false target detections. In this paper, we follow the assumption formulated in [23], in which concepts of uniform and strong mixing conditions for random sequences were utilized to assume a general disturbance model. Hence, such model can be applied to any random process satisfying a restriction on speed of decay of its auto-correlation function. This very weak restriction can be formalized as follows:

Assumption 1: [23] Let $\{c_n: \forall n\}$ be the true and thus unknown disturbance, which is a stationary discrete and circular complex valued process. Then, it is assumed that the autocorrelation function $r_C[m] \triangleq \mathbb{E}\{c_n c_{n-m}^*\}$ has a polynomial decay.

It should be noted that such assumption is sufficiently generic, and can be applied to most practical disturbance models. In fact, it is satisfied by any second order stationary (SOS) auto regressive (AR) model. Hence, it is suitable to model disturbance that is heavy tailed or compound Gaussian (CG) [29]. In order to detect the presence of targets embedded in unknown disturbance, the detection problem is formulated as binary hypothesis testing problem as described in the next subsection.

C. Detection Problem

It is assumed that the radar field of view consists of several discrete angle bins such that $\{\theta_l: l = 1, \dots, L\}$ and in total the system transmits K pulses, $k \in \{1, \dots, K\}$. The hypothesis test problem is casted as

$$H_0: \mathbf{y}_l^k = \mathbf{c}_l^k \quad k = 1, \dots, K \quad (7)$$

$$H_1: \mathbf{y}_l^k = \alpha_l^k \mathbf{h}_l + \mathbf{c}_l^k \quad k = 1, \dots, K. \quad (8)$$

Here, a composite binary hypothesis test is adopted, where the null hypothesis H_0 denotes that the cell under test contains only disturbance, i.e., clutter and noise, while the alternative H_1 denotes single target detection. As a matter of fact the entries of \mathbf{c}^k are sampled from complex random process, satisfying only the general Assumption 1, having unknown covariance matrix $\Gamma = \mathbb{E}\{\mathbf{c} \mathbf{c}^H\}$. Moreover, we assume a single snapshot scenario. In order to differentiate between H_0 and H_1 (7), a test statistic is required, where

$$\Lambda(\mathbf{y}_l^k) \stackrel{H_1}{\gtrless} \lambda. \quad (9)$$

Since in radar applications it is of fundamental importance to control the P_{FA} , the threshold λ is chosen to satisfy the following

$$\Pr\{\Lambda(\mathbf{y}_l^k) > \lambda | H_0\} = \int_{\lambda}^{\infty} p_{\Lambda|H_0}(a|H_0)da = P_{\text{FA}}, \quad (10)$$

where $p_{\Lambda|H_0}$ is the probability density function (pdf) of $\Lambda(\mathbf{y}_l^k)$ under H_0 . Usually conventional model based test statistics as *generalized likelihood ratio test (GLRT)*, or *Wald test* are used to solve for (9), yet they can not be directly applied here. This is due to the fact that the functional form of the pdf of \mathbf{c} is unknown. Instead, we apply a robust Wald-type detector derived in [23], which requires the disturbance model only to satisfy Assumption 1. This detector is asymptotically distributed, (i.e., $N \rightarrow \infty$) as chi-squared χ_2^2 random variable under both H_0 and H_1 .

This Wald-type test requires the availability of an asymptotically normal estimator of α which is \sqrt{N} consistent. This estimator can be the least squares (LS) estimator of α , which we denote here as $\hat{\alpha}$ and is given as

$$\hat{\alpha}_l = \frac{\mathbf{h}_l^H \mathbf{y}_l^k}{\|\mathbf{h}_l\|^2}. \quad (11)$$

With this in mind, the statistic of the Wald-type test for a cell under test θ_l containing a target at time k can be defined as (refer to [23] for proof)

$$\Lambda_l^k = \frac{2|\hat{\alpha}_l|^2}{\mathbf{h}_l^H \widehat{\Gamma} \mathbf{h}_l}, \quad (12)$$

where $\widehat{\Gamma}$ is the estimated value of the unknown Γ . Further details about the calculation of $\widehat{\Gamma}$, and the asymptotic distribution of Λ_l^k are provided in the Appendix.

In addition, the threshold λ in (9) is set to

$$\lambda = H_{\chi_2^2}^{-1}(P_{\text{FA}}), \quad (13)$$

with $H_{\chi_2^2}^{-1}$ is the inverse of the function $H_{\chi_2^2} = \int_{\lambda}^{\infty} p_{\Lambda_{l,g}^k}(a|H_0)da$.

The expressions in (12), and (13) are the key equations of our CR algorithm. They will be used to detect which are the cells containing targets. In the next section, we will discuss optimal way to make such decisions using reinforcement learning.

III. REINFORCEMENT LEARNING

One way to make decisions at the radar receiver is through Bayesian filtering as in [1], [2], [15]. However, this generally requires prior information about the environment, and this makes the detection algorithm prone to errors, especially in dynamic environments. Since we assume no prior knowledge about the disturbance, which is the case most frequently encountered in practice, we cannot rely on Bayesian filtering. For this reason, we propose here to adopt an approach based on reinforcement learning (RL). RL is an area of machine learning, where a learner learns the optimal way to make

decisions to achieve a certain goal. This is done by trial and error interactions with the environment [18]. This learner is often referred to as *agent*. Typically an agent performs course of actions, then it evaluates its goal achievement through two types of information received from the environment in response to those actions: its current *state*, and a *reward*. The reward is defined as a scalar feedback signal, which the agent always seeks to maximize, it is specific to a certain task and a corresponding goal [30]. The interactions with the environment in RL is formally described by Markov decision processes (MDP).

Definition 1: A Markov decision processes (MDP) is defined by a tuple $\{\mathcal{S}, \mathcal{A}, \mathcal{P}, r\}$, where \mathcal{S} is finite set of states, \mathcal{A} is a finite set of actions, \mathcal{P} is the transition probability from state s to $s' \in \mathcal{S}$ after action $a \in \mathcal{A}$ is performed, r is the immediate reward evaluated after a is executed.

Let us define *policy* $\pi: \mathcal{S} \rightarrow \mathcal{A}$ as a function which maps a state $s \in \mathcal{S}$ to action $a \in \mathcal{A}$. Moreover it defines which action to be executed at each state. Thus at time $t \in [0, T]$, the agent observes state s_t , then based on a specific policy π , it takes action $a_t = \pi(s_t)$. Consequently, a new state s_{t+1} will be reached with probability $\mathcal{P}(s_{t+1}|s_t, a_t)$, and a reward $r_{t+1} \in \mathbb{R}$ will be received. The observed information from the environment r_{t+1} , and s_{t+1} are used to adjust the policy, where this process is repeated till the optimal policy is reached. In order to estimate how good a certain state is for an agent, a *value function* $\mathcal{V}_\pi: \mathcal{S} \rightarrow \mathbb{R}$ is introduced. This function is defined as the expected cumulative reward received by agent for starting from state s , where it depends on the policy selected by the agent to execute the corresponding actions. Hence, the *state value function* for policy π is defined as

$$\mathcal{V}_\pi(s) = \mathbb{E}_\pi \left[\sum_{k=0}^{\infty} \gamma^k r_{t+k+1} | S_t = s \right], \quad (14)$$

where $\mathbb{E}_\pi [.]$ denotes the expected value of a random variable when the agent follows policy π at any time t . $\gamma \in [0, 1]$ denotes the discount factor which controls the weight given to future rewards. Hence if $\gamma = 0$ holds, then future rewards are not considered. In addition, let us define the optimal *action value function* for policy π , $Q: \mathcal{S} \times \mathcal{A} \rightarrow \mathbb{R}$ which is defined as the expected cumulative reward for starting from state s and taking action a . Hence, it differs from the *value function* because it takes the action into consideration. The *Q-function* is defined as

$$Q_\pi(s, a) = \mathbb{E}_\pi \left[\sum_{k=0}^{\infty} \gamma^k r_{t+k+1} | s_t = s, a_t = a \right], \quad (15)$$

therefore the optimal *value function* can be written as

$$\mathcal{V}_\pi^*(s) = \arg \max_{a \in \mathcal{A}} Q_\pi(s, a). \quad (16)$$

In the next section will map the aforementioned RL results into our MMIMO radar setup.

IV. RL-BASED MMIMO COGNITIVE RADAR

In this section, we apply the above results of reinforcement learning to the MMIMO multi-target detection scenario, based on the problem formulated in Sect. II.

A. The set of states

To define the state space \mathcal{S} , the statistic Λ_l^k from eq. (12) is utilized. If Λ_l^k is greater than the defined threshold λ from eq. (13) for the angle bin l at time k , a new statistic $\bar{\Lambda}_l^k$ is set to 1, otherwise it is 0.

$$\bar{\Lambda}_l^k = \begin{cases} 1 & \Lambda_l^k > \lambda \\ 0 & \text{otherwise.} \end{cases} \quad (17)$$

That basically means it indicates whether or not it is likely for the angle bin l to contain a target. Hence state s_k is then defined as the total number of angle bins where the targets could be located at time t :

$$s_k = \sum_l^L \bar{\Lambda}_l^k. \quad (18)$$

There is a maximum number of targets γ , which the MIMO radar can identify [24]. Hence, the set of possible states can be written as $\mathcal{S} = \{0, \dots, \gamma\}$.

B. The set of actions

A MIMO radar agent performs an action $a \in \mathcal{A} = \{a_i | i \in \{1, 2, \dots, \gamma\}\}$ over two consecutive steps:

1) *Data Acquisition*: A received signal snapshot \mathbf{y}_t^k as defined in (5) is collected at time step k . Afterwards, the set $\Theta_i = \{\hat{\theta}_1, \dots, \hat{\theta}_i\} \subset \mathcal{L}$ is specified which has i angle bins that most likely contain targets. In order to identify Θ_i , the highest i values of Λ_l^k , defined in (12), are calculated and the respective angles are extracted. We define the set of indices i as

$$\mathcal{T}_i = \arg\max_{l \in \{0, \dots, L-1\}} \Lambda_l^k. \quad (19)$$

The indices of the i angle bins are in the set \mathcal{T}_i and the respective angle bins are in the set \mathcal{L} which can be expressed as $\Theta_i = \{\hat{\theta}_j \in \mathcal{L} | j \in \mathcal{T}_i\}$.

2) *Beamforming*: The weighting matrix \mathbf{W} has to be optimized, in order to synthesize the corresponding beam pattern. Therefore, the transmitted power is concentrated towards those angle bins in Θ_i , which may contain targets.

This is done by maximizing the minimum of the beam pattern $B(\hat{\theta}_j) = \mathbf{a}_T^T(\hat{\theta}_j) \mathbf{R}_W \mathbf{a}_R^*(\hat{\theta}_j)$, with $\mathbf{R}_W = \mathbf{W} \mathbf{W}^H$, $\hat{\theta}_j \in \Theta_i$ and under the power constraint $\text{tr}(\mathbf{R}_W) = P_T$. The resulting optimization problem is stated as follows:

$$\begin{aligned} \max_{\mathbf{W}} \min_{j \in \mathcal{T}_i} \{ \mathbf{a}_T^T(\hat{\theta}_j) \mathbf{W} \mathbf{W}^H \mathbf{a}_R^*(\hat{\theta}_j) \} \\ \text{s.t. } \text{tr}(\mathbf{W} \mathbf{W}^H) = P_T. \end{aligned} \quad (20)$$

Details of the optimization problem and its solution are provided in Sect. V.

C. The reward

The reward defines the goal of the RL problem, hence the radar agent's sole objective is to maximize the total cumulative reward function on the long run [18]. Consequently, it defines how the agent should behave, as the agent learns what are the good and bad actions. In our case, the goal is to detect all the targets even those masked within the disturbance.

This is achieved through specific actions, i.e., optimizing the beampattern. Therefore, the reward is expressed in terms of the estimated \hat{P}_D as

$$\hat{P}_D = Q_1 \left(\sqrt{\hat{\zeta}}, \sqrt{\lambda} \right), \quad (21)$$

$$\hat{\zeta} = 2|\hat{\alpha}|^2 \frac{\|\mathbf{h}\|^4}{\mathbf{h}^H \hat{\Gamma} \mathbf{h}}, \quad (22)$$

where $Q_1(.,.)$ is first order *Marcum Q function* [31], $\hat{\alpha}$ is defined in (11), and $\hat{\Gamma}$ is defined as in (39). The reward expression is composed of two parts, negative and positive reward. The negative reward can be considered as penalty for the agent in case of false detections. Hence, the positive reward is the summation of \hat{P}_D for the angle cells defined in i . While the negative reward is the summation of \hat{P}_D for the rest of the cells, which is likely not to contain any target. The reward for each timestep k will be defined as:

$$r_{k+1} = \sum_{l=1}^i (\hat{P}_D)_l^k - \sum_{j=1}^{L-i} (\hat{P}_D)_j^k. \quad (23)$$

In order to guide the agent and its interactions with the environment, we use the SARSA algorithm. The acronym SARSA is derived from the *state-action-reward-state-action* sequence to update the Q-values [32], which is explained in the next subsection.

D. MIMO radar SARSA algorithm

SARSA is an on-policy RL algorithm, meaning that after the agent interacts with the environment, the policy is updated based on the actions taken, then the *Q-function* is updated accordingly. It falls under the category of model-free reinforcement learning algorithms, because it does not require a model of the environment. In the SARSA algorithm, the agent has to maintain a \mathbf{Q} matrix of elements $Q(s_k, a_k)$, initialized with 0, afterwards based on the execution of a certain action, the agent shifts from one state to another, then updates the *Q-function*. Hence, the *Q-function* depends on the quintuple $(s_k, a_k, r_{k+1}, s_{k+1}, a_{k+1})$. This means that if the agent is in state s_k , then performed action a_k , it will receive reward r_{k+1} . Hence, it will end up in state s_{k+1} , consequently it will decide to execute the next action a_{k+1} . This iteration is used to update $Q(s_k, a_k)$ according to the following update rule [18]

$$\begin{aligned} Q(s_k, a_k) &\leftarrow Q(s_k, a_k) + \\ &\alpha (r_{k+1} + \gamma Q(s_{k+1}, a_{k+1}) - Q(s_k, a_k)) \end{aligned} \quad (24)$$

The learning rate $\alpha \in [0, 1]$ is used to control how much the recent experiences override the old ones. For instance, as α increases, the influence of the recent experiences on the *Q function* increases.

E. Exploration vs Exploitation

One challenge in designing RL algorithms, is the trade off between exploration and exploitation. In more details, the agent must follow the same actions which was tried in the past and proved to maximize the reward. However, the agent is

Algorithm 1 SARSA

Initialize $Q(s, a)$ with zeros
 Initialize state $s_0 = 0$, $\mathbf{W} = \mathbf{I}$
repeat for each time step:
 Acquire the received signal \mathbf{y}_l^k
 Calculate s_k from (18)
 Define \mathcal{T}_i from (19)
 Choose action a_k from s_k using policy derived from Q (e.g., ϵ -greedy)
 Solve for \mathbf{W} in (20) using algorithm (2)
 Take action a_k by transmitting waveform in (2)
 Observe reward r_{k+1} as in (23) and next state s_{k+1}

$$Q(s_k, a_k) \leftarrow Q(s_k, a_k) + \alpha (r_{k+1} + \gamma Q(s_{k+1}, a_{k+1}) - Q(s_k, a_k))$$

$$s_k \leftarrow s_{k+1}; a_k \leftarrow a_{k+1}$$

until s is terminal

required also to acquire new knowledge through discovering new actions. Hence, the agent remains in a dilemma whether to exploit the existing experience, or explore a new one for the aim of finding better actions. One strategy to address this problem is the ϵ -greedy. This strategy selects a new action based on the previous observations (in our case: the Q -function) as explained in algorithm (1). The optimal action a_{opt} (highest value in Q) is taken with a probability of $1 - \epsilon$, while another random action a_{rnd} (excluding a_{opt}) is chosen with a probability of ϵ such that

$$a_t = \begin{cases} a_{\text{opt}} & \text{withprob. } 1 - \epsilon \\ a_{\text{rnd}} & \text{withprob. } \epsilon. \end{cases} \quad (25)$$

This implies if we set $\epsilon = 0$, the agent will not explore anything, and would always choose a_{opt} . Whereas, if we set $\epsilon = 1$, the action is selected randomly, and the agent would not exploit the information previously learned and saved in the Q -function.

V. OPTIMIZATION PROBLEM

Semi-definite programming (SDP) relaxation is a widely used method to solve the optimization problem (20) [24], [25], [33], however SDP complexity increases with the size of \mathbf{W} , hence using SDP for the MMIMO application previously described would not be realistic. Moreover, SDP involves a relaxation of the original problem and getting a feasible solution requires a heuristic randomization process. The high complexity of the solution described in [25], [34], [35] to the optimization problem is due to its two-steps structure: in the first step, \mathbf{R}_W is synthesized; then in the second step, the beamformer matrix \mathbf{W} is generated from \mathbf{R}_W . To reduce the computational complexity, we propose another approach based on outer convex approximations (OCA) [36]. This allows to find directly \mathbf{W} , iteratively. This guarantees obtaining a stationary point satisfying the first order optimality of the

original problem and avoids rank relaxation issues of the SDP approach. Hence, (20) can be written as follows

$$\max_{\mathbf{W}, \zeta} \zeta \quad (26)$$

$$\text{s. t. } \zeta \geq 0, \text{ tr}(\mathbf{W}^H \mathbf{W}) = P_T \quad (27)$$

$$\mathbf{a}_T^T(\hat{\theta}_j) \mathbf{W} \mathbf{W}^H \mathbf{a}_R^*(\hat{\theta}_j) \geq \zeta, \forall j \in \mathcal{T}_i. \quad (28)$$

Problem (26) is non-convex and difficult to solve due to constraints in (28). To overcome this difficulty, we propose to iteratively approximate the non-convex feasible set with a convex feasible set by approximating the function $f_j(\mathbf{W}) \triangleq \mathbf{a}_T^T(\hat{\theta}_j) \mathbf{W} \mathbf{W}^H \mathbf{a}_R^*(\hat{\theta}_j)$ with its first-order Taylor series representation. This outer approximation approach, iteratively enhances the lower-bound on the convex function $f_j(\mathbf{W})$ and eventually converges to a stationary solution of problem (26). Let i be iteration index and \mathbf{W}^i be the beam-forming matrix at iteration i . The first order approximation of the function $f_j(\mathbf{W})$ writes

$$\tilde{f}_j(\mathbf{W}; \mathbf{W}^j) = f_j(\mathbf{W}^i) + \langle \nabla_{\mathbf{W}} f_j(\mathbf{W}^i), \mathbf{W} - \mathbf{W}^i \rangle, \quad (29)$$

where $\nabla_{\mathbf{W}} f_j(\mathbf{W}^i)$ is the gradient of function $f_j(\mathbf{W})$ with respect to \mathbf{W} computed at \mathbf{W}^i and $\langle \mathbf{A}, \mathbf{B} \rangle = \text{tr}(\mathbf{A}^H \mathbf{B})$. The successive lower-bound approximation approach is based on solving the following problem iteratively until convergence

$$\max_{\mathbf{W}, \zeta} \zeta \quad (30)$$

$$\text{s. t. } \zeta \geq 0, \text{ tr}(\mathbf{W}^H \mathbf{W}) = P_T \quad (31)$$

$$\tilde{f}_j(\mathbf{W}; \mathbf{W}^j) \geq \zeta, \forall j \in \mathcal{T}_i, \quad (32)$$

Problem (30) is convex and the optimal solution can be found efficiently with an interior-point solver such as in [37]. The algorithm for finding the stationary solution of problem (26) is listed in algorithm 2.

Algorithm 2 Iterative Outer Convex Approximation Algorithm

Set $i = 0$ and initialize \mathbf{W}^0 such that $\text{tr}((\mathbf{W}^0)^H \mathbf{W}^0) = P_T$.
 Repeat until convergence:
 Solve problem (30) approximated around point \mathbf{W}^i .
 Set \mathbf{W}^{i+1} as the optimal solution of problem (30)
 $i \leftarrow i + 1$

VI. NUMERICAL ANALYSIS

In this section, the cognitive MIMO radar using the SARSA algorithm is simulated, where the agent is in a continuous learning mode of the surrounding environment, taking decisions while learning. The performance is averaged over multiple Monte Carlo runs. Table I summarizes the values of the parameters for the SARSA algorithm.

Parameter	Value	Parameter	Value
Learning rate α	0.8	Discount factor γ	0.8
exploration rate ϵ_0	0.5	Time steps	50
Number of states	11	Initial state	1
Number of actions	11		

Table I: Reinforcement learning parameters

A. Simulation Setup

In our simulations, we consider a uniform linear array (ULA) at the transmitter and receiver each with inter-element spacing of d . The angle grid is divided into $L = 20$ angle bins. The angular locations would be represented in terms of the spatial frequency ν , which is defined as

$$\nu \triangleq \frac{df_c}{V_c} \sin(\theta) \quad (33)$$

where f_c is the carrier frequency, and V_c is the speed of light. Hence, the steering vector for the transmit or receive can be redefined in terms of ν

$$\mathbf{a}_R(\theta) = [1, e^{j2\pi\nu}, \dots, e^{j2\pi(N-1)\nu}]^T, \quad (34)$$

where N is the number of transmit or receive antennas. Furthermore, the angle grid can be expressed as a spatial frequency grid where $\nu = [-0.5 : 0.45]$. We further assume the existence of four targets at spatial frequency locations $\nu = \{-0.2, 0, 0.2, 0.3\} \subset \nu$, with $\text{SNR} = [-5\text{dB}, -8\text{dB}, -10\text{dB}, -7\text{dB}]$ respectively.

B. Disturbance Model

The disturbance model was chosen to mask the target angles, where the disturbance power is spread all over the spatial frequency range. Hence, the potential of our RL cognitive radar algorithm can be analyzed in such harsh environment. The disturbance \mathbf{c} was generated according to the model of circular SOS AR(p) [23] as

$$c_n = \sum_{i=1}^p \rho_i c_{n-i} + w_n, \quad n \in (-\infty, \infty), \quad (35)$$

where $p = 6$, driven by identically independent (i.i.d.), t -distributed innovations w_n . p_w is the pdf of w_n is defined as [23], [38] :

$$p_w(w_n) = \frac{\mu}{\sigma_w^2} \left(\frac{\mu}{\xi} \right)^\mu \left(\frac{\mu}{\xi} + \frac{|w_n|^2}{\sigma_w^2} \right)^{-(\mu+1)}. \quad (36)$$

$\mu \in (1, \infty)$ is the shape parameter controlling p_w tails, where if $\mu \rightarrow 1$, then p_w is a heavy tailed pdf with highly non-Gaussian distribution. However, the pdf becomes Gaussian if $\mu \rightarrow \infty$. The scale parameter is defined by $\xi = \mu / (\sigma_w^2 (\mu - 1))$. We set in our simulations $\mu = 2$ and $\sigma_w^2 = 1$. Hence, the normalized power spectral density (PSD) of the disturbance is given by [23]

$$S(\nu) \triangleq \sigma_w^2 \left| 1 - \sum_{n=1}^p \rho_n e^{-j2\pi\nu} \right|^{-2}, \quad p = 6. \quad (37)$$

The coefficient vector ρ is defined as

$$\rho = [0.5e^{-j2\pi 0.4}, 0.6e^{-j2\pi 0.2}, 0.7e^{-j2\pi 0}, 0.4e^{-j2\pi 0.1}, 0.5e^{-j2\pi 0.3}, 0.6e^{-j2\pi 0.35}]^T. \quad (38)$$

The disturbance PSD is shown in Fig.1, where the target angles are marked in red dashed lines. Note that the disturbance PSD has multiple peaks.

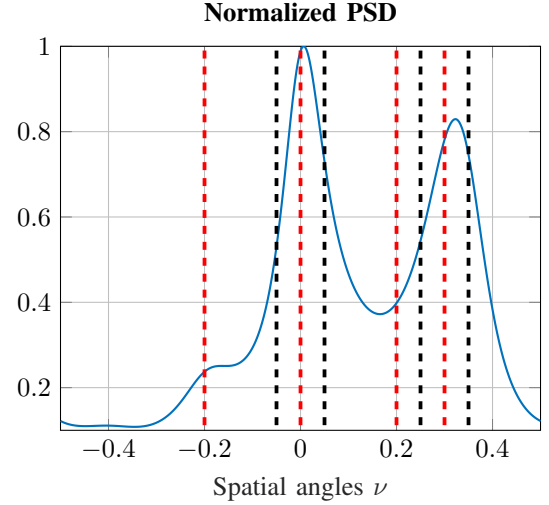


Figure 1: Disturbance PSD along with targets angles locations (red dashed lines for study case 1, and blue ones for study case 2)

C. Study Case 1 : Stationary Environment

To exploit the benefits of RL, we compared the the proposed RL-based beamformer against omnidirectional equal power allocation with no RL. In this case all antennas emit orthogonal waveforms, and the power is divided equally across all antennas. It is assumed that the total power $P_T = 1$ in both cases. For fair comparison, the same detector is used in both cases according to (17) in each time step. In this set of simulations, the environment is assumed to be temporally stationary. The difference in behavior of the MMIMO radar with / without RL is analyzed. The results were averaged over 10^4 Monte Carlo runs.

1) *Scenario 1*: In this scenario, the performance of the algorithm is analyzed for a MMIMO regime where $N = N_T N_R = 10^4$, and $P_{\text{FA}} = 10^{-5}$. Fig. 2 depicts the difference between our proposed algorithm and omnidirectional MIMO. In order to produce those figures, we calculated the threshold in (17) within each time step, then the average was taken across all Monte Carlo runs. Fig.2a demonstrates better detection performance for all targets even the ones with low SNR. It can be shown that the algorithm learns across time, where in the first ten time steps, the agent is learning the disturbance, enhancing its experience as the time passes. Conversely, in the omnidirectional approach in Fig.2b the targets with lower SNR are mostly masked under the disturbance peaks, as in the case of $\nu = 0$ and $\nu = 0.3$. To measure the convergence of our algorithm, we calculated the immediate reward function as in (23). In fact, it shows similar behavior to Fig.2a, where the reward function converges after 10 time steps. Since the agent learns all the targets' locations after gathering experience from the environment which is represented in the Q table constructed over time in (24).

2) *Scenario 2*: In this scenario we simulated the P_D estimated from the closed form expression in (21) as a function of the spatial virtual antenna channels N . Here, the number of transmit and receive antennas are $N_T = N_R =$

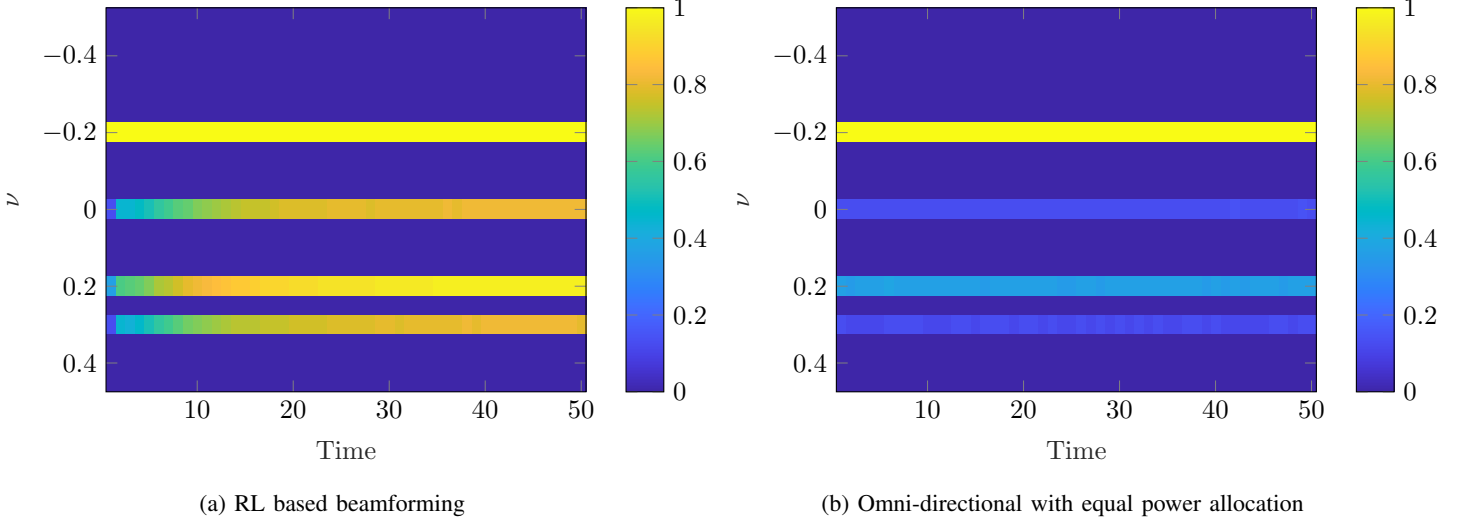


Figure 2: Detection performance of proposed RL beamforming vs. omnidirectional with equal power allocation under $P_{\text{FA}} = 10^{-5}$ and $N = N_T N_R = 10^4$.

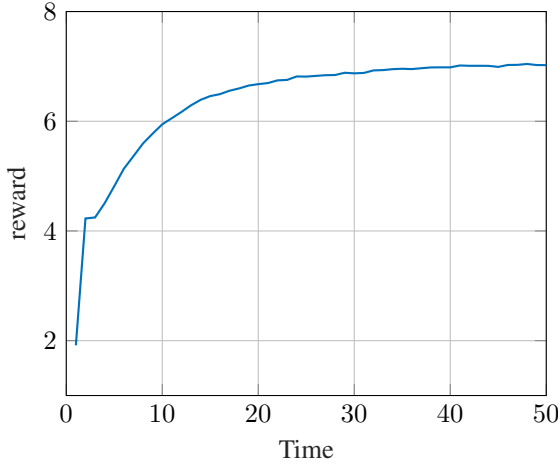


Figure 3: Reward calculated as in (23) for RL-based beamformer with $P_{\text{FA}} = 10^{-5}$ and $N = N_T N_R = 10^4$.

[10, 12, 16, 21, 27, 35, 46, 59, 77, 100].

The results in Fig. 4 show that as N increases, the P_D increases for all the targets. However, the suggested algorithm provides better performance than the omni-directional case. The low P_D as $N \rightarrow 10^3$ shown in Fig. 4b, 4c and 4d, is due to the harsh operating conditions, since $P_T = 1$, and the nominal $P_{\text{FA}} = 10^{-4}$. Furthermore, the corresponding targets are located within heavy disturbance.

3) *Scenario 3*: In this scenario, the receiver operating characteristics curve (ROC) is simulated across a range of $P_{\text{FA}} = [10^{-5}, 10^{-4}, 10^{-3}, 10^{-2}, 1]$ with $N = 10^4$. As shown in Fig. 5, mainly the potential of the RL-based cognitive MMIMO radar is shown in low P_{FA} regimes. As a matter of fact most practical radar applications has to maintain preassigned low P_{FA} values. Hence, we conclude that our proposed algorithm is more suitable for those practical systems in general. Meanwhile, it is notably visible from Fig. 5a, that

the P_D is 1 across all P_{FA} . This is due to the fact that this target has relatively high SNR, and located within relatively low disturbance PSD. This means that omnidirectional systems can perform well in those conditions. Meanwhile, the P_D for targets with low SNR is much higher for the proposed algorithm compared to the omni directional solution, i.e., $\nu = 0$ in Fig. 5b, $\nu = 0.2$ in Fig. 5c. For both algorithms, P_D approaches 1 for as the $P_{\text{FA}} \rightarrow 1$.

D. Dynamic Environment

In these simulations, the environment changes and the performance of our algorithm is analyzed such that the radar agent capability to adapt to those changes is tested. The number of total time steps is 100, and the results are averaged over 1000 Monte Carlo runs.

1) *Scenario 4 : Changing Spatial frequencies*: In this scenario, the targets' spatial frequencies are changed after 50 time steps. In this case ν was changed from $[-0.2, 0, 0.2, 0.3]$ to $[-0.05, 0.05, 0.1, 0.25, 0.35]$ where the new spatial frequencies are depicted in dashed blue in Fig.1. In this case, we aim at simulating a dynamic environment as shown in Fig. 6, while their respective SNR remains the same, where $N = 10^4$ and $P_{\text{FA}} = 10^{-5}$. On one hand, Fig. 6b shows the performance of the omnidirectional case, where it can detect only targets whose new spatial frequencies are located where the disturbance PSD is low, i.e., $\nu = 0.1$. On the other hand, the RL based beamforming algorithm can detect all the targets, even those lying close to the disturbance PSD peaks. Similar to scenario 1, Fig. 7 shows the reward behavior across time as calculated in (23) and averaged over the Monte Carlo runs. The reward shows convergence after $T = 20$ time steps. Then when the environment is changed by changing the angles, the agent sensed that change through exploration. Hence, the drop in the reward is seen after $T = 50$ time steps, where the agent starts re-learning the changes, then after 10 time steps, the reward converges again.

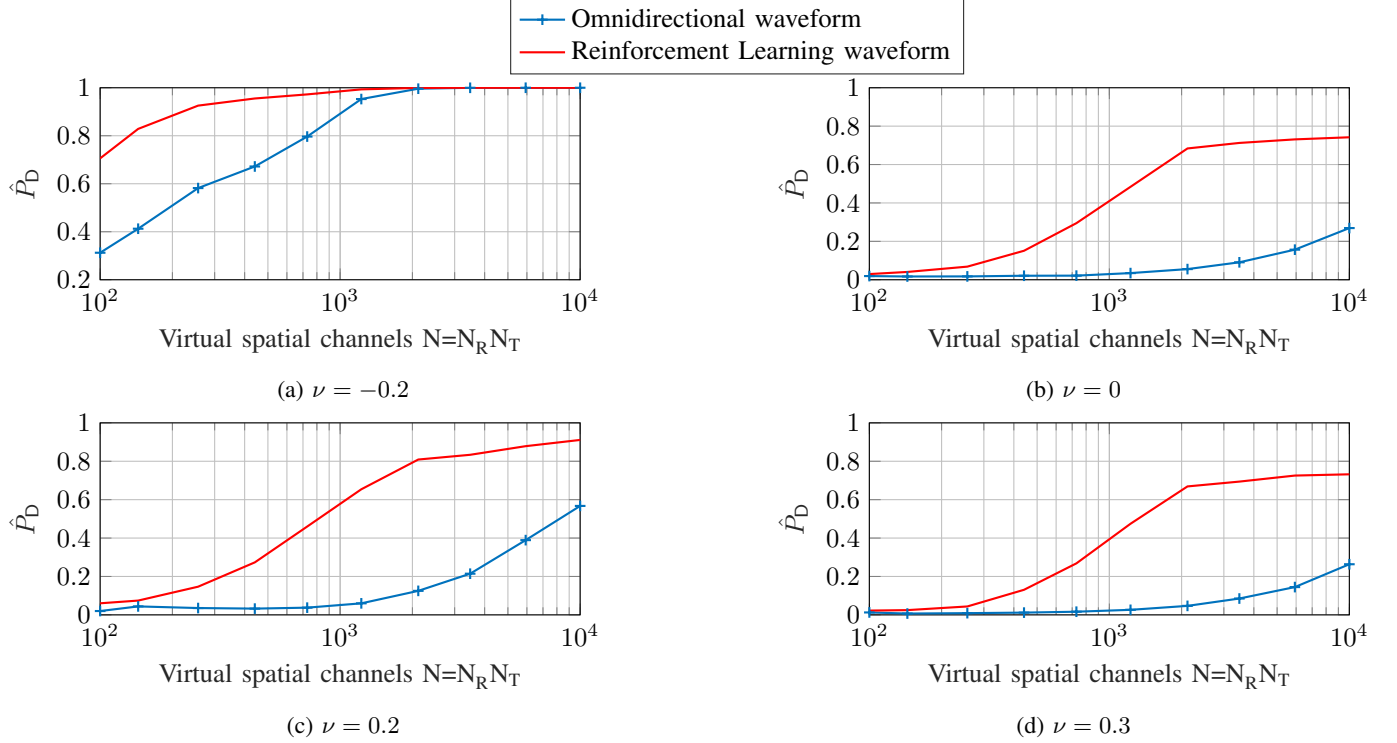


Figure 4: \hat{P}_D with RL of existing targets across different virtual antenna array size with $P_{FA} = 10^{-4}$ a) spatial angle -0.2 with SNR = -5 dB b) spatial angle 0 with SNR = -8 dB c) spatial angle 0.2 with SNR = -10 dB d) spatial angle 0.3 with SNR = -7 dB.

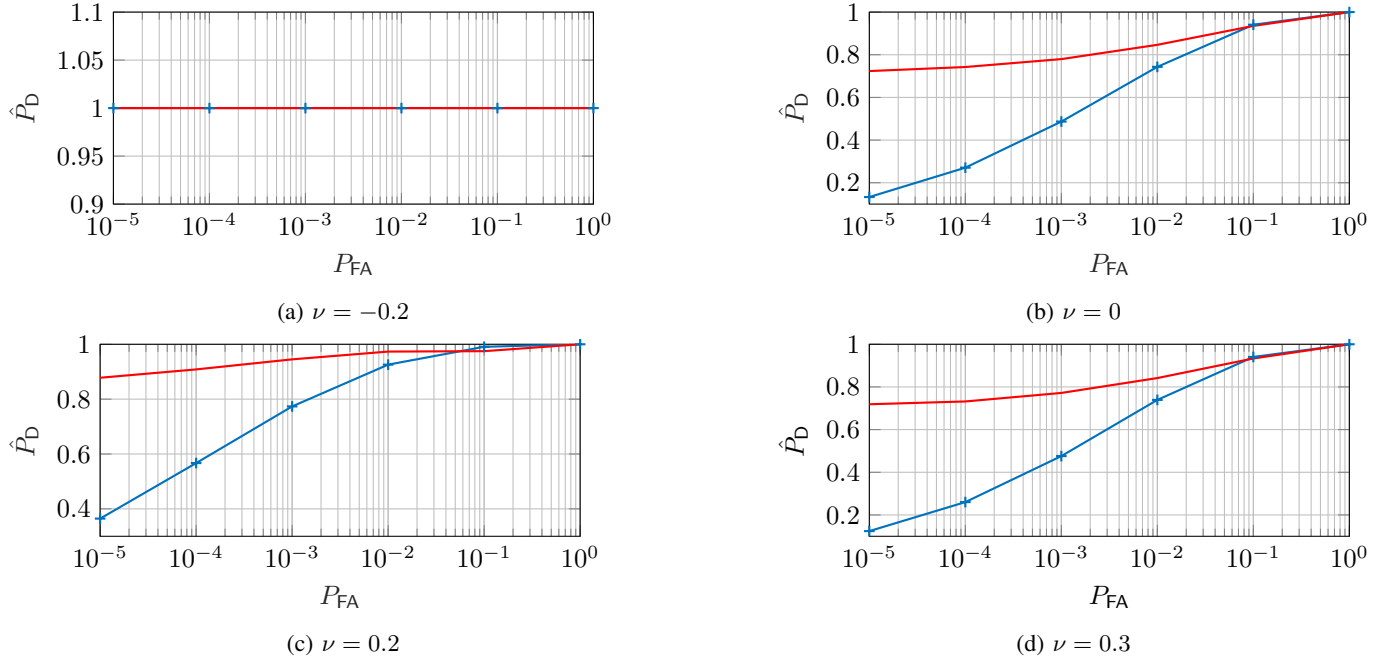


Figure 5: \hat{P}_D of existing targets across different P_{FA} with $N = 10^4$ a) spatial angle -0.2 with SNR = -5 dB b) spatial angle 0 with SNR = -8 dB c) spatial angle 0.2 with SNR = -10 dB d) spatial angle 0.3 with SNR = -7 dB.

2) *Scenario 5: Fading Targets:* Here we simulate a different change in the environment, where we assume that the targets are fading, and their SNR is decreasing. In Fig. 8, the targets' SNRs are assumed to decrease by 20% every 30 time steps.

Hence, by $T = 90$, all targets' SNRs would have decreased by 60%. In Fig. 8b, the omnidirectional approach could not detect most of the targets after the first 30 time steps. Furthermore, the first target located at $\nu = -0.2$, which proved very good

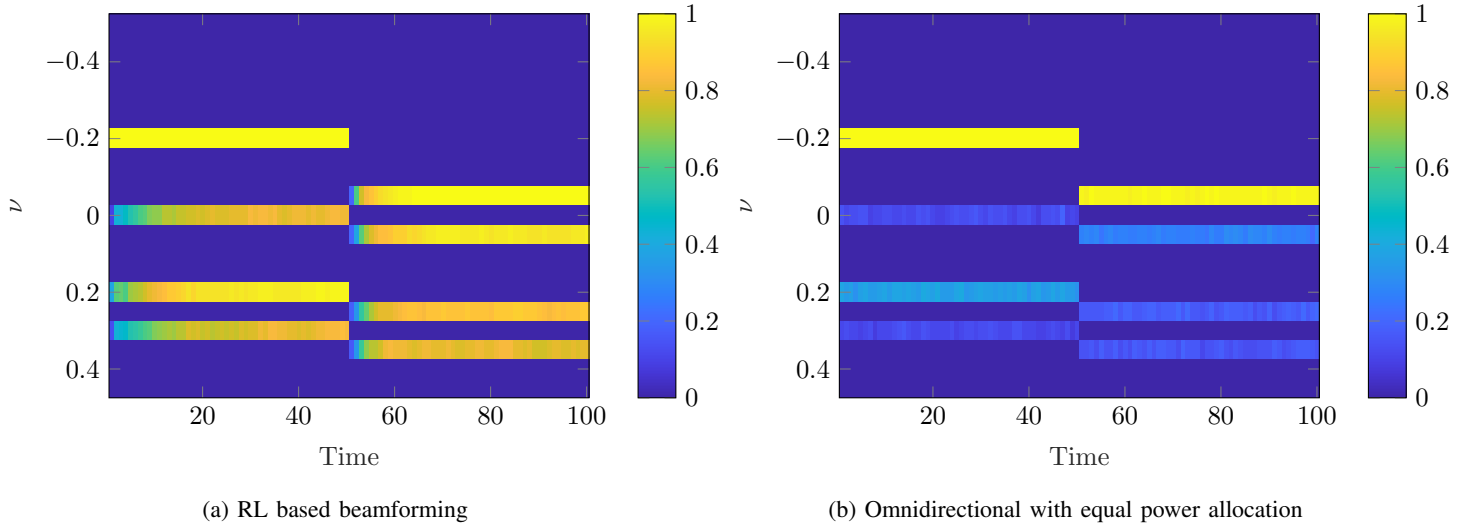


Figure 6: Detection performance of Omnidirectional with equal power allocation vs RL based beamforming for dynamic environment: changing angles at $T = 50$.

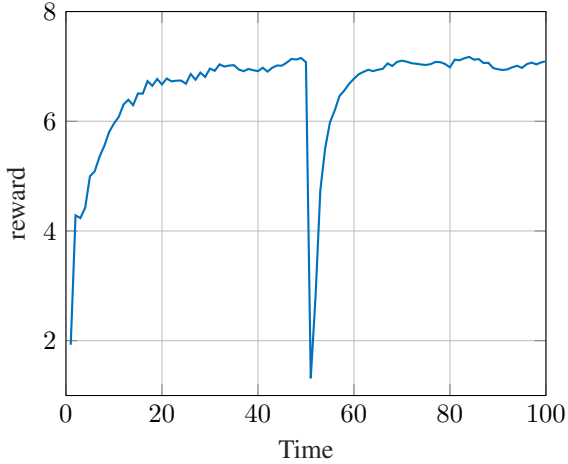


Figure 7: RL reward in dynamic environments: changing angles at $T = 50$.

performance in the previous simulations due to its good SNR starts fading at $T = 90$. This proves that the omnidirectional approach fails in the fading scenarios, since the radar here does not learn anything from the environment unlike in the RL case. Hence, it can not adapt to such changes. However, our proposed RL based beamforming algorithm obviously proves to have a reliable performance across the entire time steps. It can be concluded that RL cognitive MMIMO radar can adapt very well to all the environmental changes with very good performance. The corresponding reward behavior is shown in Fig.9, where the algorithm can adapt to those changes in the SNR without any convergence issues.

VII. CONCLUSION

In this paper, we studied the problem of multi-target detection for a MMIMO CR in the presence of unknown disturbance. We proposed a novel RL based beamforming

algorithm, which could detect the targets with very low SNR even if the environment is dynamic. Specifically, the CR acted as an agent sensing the unknown environment (i.e., targets and disturbance) through illuminating it by transmitting a waveform. Afterwards, a reward function was calculated from the reflected echoes. This reward has been defined as the closed form asymptotic expression of the P_D as the number of virtual spatial antenna channels N go to infinity. The agent's goal was to maximize the reward through a course of actions without any a priori knowledge about the disturbance distribution, nor the targets number. In our case, those actions were tailoring the beampattern by optimizing the beamformers according to the acquired knowledge. Furthermore, we presented a novel approach for beamforming optimization, which is scalable as the size of N increases, and does not increase the complexity. Our numerical results showed a really good P_D performance for our algorithm as $N \rightarrow 10^4$ compared to the omnidirectional approach with equal power allocation. In addition, the ROC confirmed the advantages of adopting a RL-based approach when the targets are embedded in spatially correlated heavy-tailed disturbance. The probability of detecting the low- SNR targets improves significantly. Moreover, a dynamic environment has been simulated by changing target angles and simulating target fading. In both cases, the proposed RL-based beamformer was able to adapt to the fast changing environment, without any a priori knowledge, and to provide better performance than the classical (omnidirectional) beamformer.

APPENDIX

In general, the disturbance statistics Γ is unknown. Hence according to [23, Remark 1], an estimate of the entries of Γ are given by

$$[\hat{\Gamma}_l]_{i,j} = \begin{cases} \hat{c}_i \hat{c}_j^* & j - i \leq l \\ \hat{c}_i^* \hat{c}_j & i - j \leq l \\ 0 & |i - j| > l \end{cases} \quad (39)$$

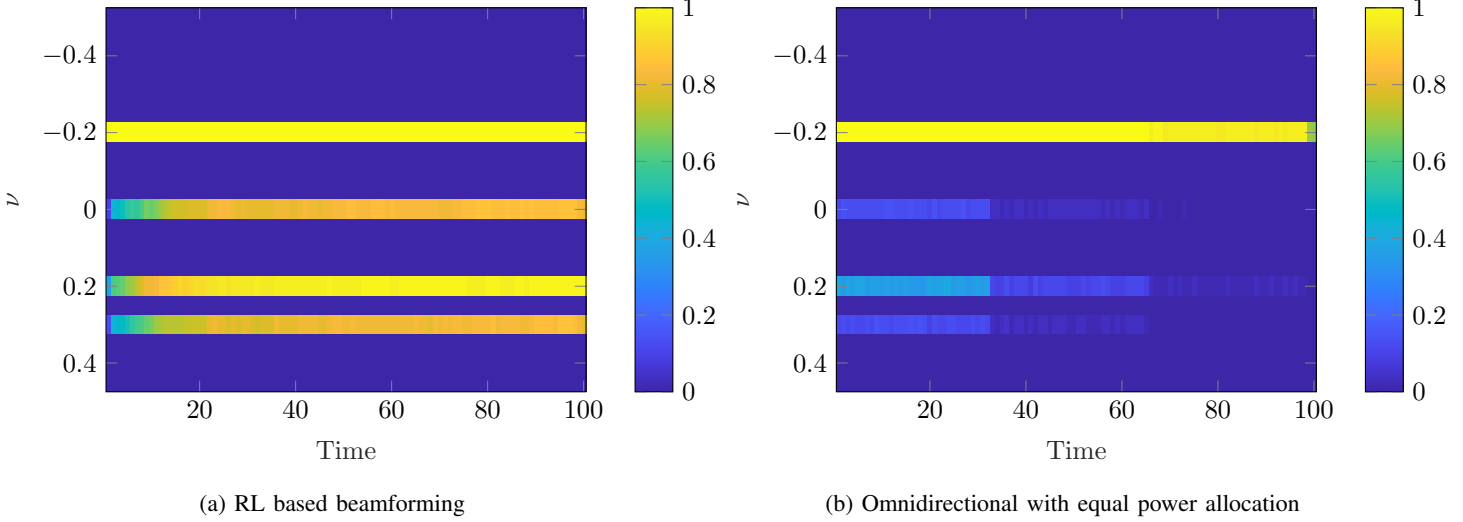


Figure 8: Detection performance of Omnidirectional with equal power allocation vs RL based beamforming for dynamic environment i.e., target's SNR decreases by 20 % every 30 time steps.

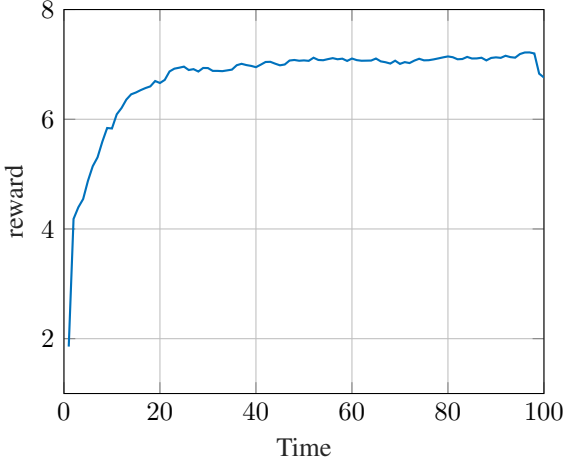


Figure 9: RL reward in dynamic environments: fading targets.

where l is the truncation lag [39], and $\hat{c} = y_n - \hat{a}h_n$. Generally speaking, if Assumption 1 holds, then the asymptotic distribution under H_0 and H_1 of the Wald statistic is

$$\Lambda_l^k(\mathbf{y}_{l,g}^k | H_0) \xrightarrow[N_T N_R \rightarrow \infty]{} \chi_2^2(0), \quad (40)$$

$$\Lambda_l^k(\mathbf{y}_{l,g}^k | H_1) \xrightarrow[N_T N_R \rightarrow \infty]{} \chi_2^2(\zeta), \quad (41)$$

where

$$\zeta = 2|\alpha|^2 \frac{\|\mathbf{h}\|^4}{\mathbf{h}^H \mathbf{T} \mathbf{h}}. \quad (42)$$

Furthermore, under asymptotic detection performance of (41), a closed form expression for P_D can be formulated as

$$P_D(\lambda) \rightarrow_{N \rightarrow \infty} Q_1\left(\sqrt{\zeta}, \sqrt{\lambda}\right), \quad (43)$$

where $Q_1(\cdot, \cdot)$ is first order *Marcum Q function* [31].

REFERENCES

- [1] S. Haykin, "Cognitive radar: a way of the future," *IEEE Signal Processing Magazine*, vol. 23, no. 1, pp. 30–40, Jan 2006.
- [2] S. Haykin, Y. Xue, and P. Setoodeh, "Cognitive radar: Step toward bridging the gap between neuroscience and engineering," *Proceedings of the IEEE*, vol. 100, no. 11, pp. 3102–3130, Nov 2012.
- [3] J. R. Guerci, "Cognitive radar: A knowledge-aided fully adaptive approach," in *2010 IEEE Radar Conference*, May 2010, pp. 1365–1370.
- [4] A. M. Haimovich, R. S. Blum, and L. J. Cimini, "MIMO radar with widely separated antennas," *IEEE Signal Processing Magazine*, vol. 25, no. 1, pp. 116–129, 2008.
- [5] J. Li and P. Stoica, "MIMO radar with colocated antennas," *IEEE Signal Processing Magazine*, vol. 24, no. 5, pp. 106–114, Sep. 2007.
- [6] P. Stoica, J. Li, and Y. Xie, "On probing signal design for MIMO radar," *IEEE Transactions on Signal Processing*, vol. 55, no. 8, pp. 4151–4161, Aug 2007.
- [7] D. W. Bliss and K. W. Forsythe, "Multiple-input multiple-output (MIMO) radar and imaging: degrees of freedom and resolution," in *The Thirty-Seventh Asilomar Conference on Signals, Systems Computers*, 2003, vol. 1, Nov 2003, pp. 54–59 Vol.1.
- [8] J. Li, P. Stoica, L. Xu, and W. Roberts, "On parameter identifiability of MIMO radar," *IEEE Signal Processing Letters*, vol. 14, no. 12, pp. 968–971, Dec 2007.
- [9] A. M. Ahmed, A. Alameer, D. Erni, and A. Sezgin, "Maximizing information extraction of extended radar targets through MIMO beamforming," *IEEE Geoscience and Remote Sensing Letters*, vol. 16, no. 4, pp. 539–543, April 2019.
- [10] T. L. Marzetta, "Noncooperative cellular wireless with unlimited numbers of base station antennas," *IEEE Transactions on Wireless Communications*, vol. 9, no. 11, pp. 3590–3600, November 2010.
- [11] Huawei. Huawei launches 5g simplified solution. [Online]. Available: <https://www.huawei.com/en/press-events/news/2019/2/huawei-5g-simplified-solution>
- [12] E. Björnson, L. Sanguinetti, H. Wymeersch, J. Hoydis, and T. L. Marzetta, "Massive MIMO is a reality—what is next?: Five promising research directions for antenna arrays," *Digital Signal Processing*, vol. 94, pp. 3 – 20, 2019, special Issue on Source Localization in Massive MIMO.
- [13] J. Ochodnický, Z. Matousek, M. Babjak, and J. Kurty, "Drone detection by Ku-band battlefield radar," in *2017 International Conference on Military Technologies (ICMT)*, May 2017, pp. 613–616.
- [14] M. S. Greco, F. Gini, P. Stinco, and K. Bell, "Cognitive radars: On the road to reality: Progress thus far and possibilities for the future," *IEEE Signal Processing Magazine*, vol. 35, no. 4, pp. 112–125, 2018.
- [15] K. L. Bell, C. J. Baker, G. E. Smith, J. T. Johnson, and M. Rangaswamy, "Cognitive radar framework for target detection and tracking," *IEEE Journal of Selected Topics in Signal Processing*, vol. 9, no. 8, pp. 1427–1439, Dec 2015.

- [16] P. Liu, Y. Liu, T. Huang, Y. Lu, and X. Wang, "Cognitive radar using reinforcement learning in automotive applications," *CoRR*, vol. abs/1904.10739, 2019. [Online]. Available: <http://arxiv.org/abs/1904.10739>
- [17] F. Zhou, D. Zhou, and G. Yu, "Target tracking in interference environments reinforcement learning and design for cognitive radar soft processing," in *2008 Congress on Image and Signal Processing*, vol. 4, May 2008, pp. 73–77.
- [18] R. S. Sutton and A. G. Barto, *Reinforcement Learning: An Introduction*, 2nd ed. The MIT Press, 2018. [Online]. Available: <http://incompleteideas.net/book/the-book-2nd.html>
- [19] W. Jiang, A. M. Haimovich, and O. Simeone, "End-to-end learning of waveform generation and detection for radar systems," in *53rd Asilomar Conference on Signals, Systems, and Computers*, 2019, pp. 1672–1676.
- [20] J. Metcalf, S. D. Blunt, and B. Himed, "A machine learning approach to cognitive radar detection," in *2015 IEEE Radar Conference (RadarCon)*, May 2015, pp. 1405–1411.
- [21] A. Guerra, F. Guidi, D. Dardari, and P. M. Djurić, "Reinforcement learning for uav autonomous navigation, mapping and target detection," May 2020.
- [22] H. Jiang, Y. Lu, and S. Yao, "Random matrix based method for joint DOD and DOA estimation for large scale MIMO radar in non-Gaussian noise," in *2016 IEEE International Conference on Acoustics, Speech and Signal Processing (ICASSP)*, March 2016, pp. 3031–3035.
- [23] S. Fortunati, L. Sanguinetti, F. Gini, M. S. Greco, and B. Himed, "Massive MIMO radar for target detection," *IEEE Transactions on Signal Processing*, vol. 68, pp. 859–871, 2020.
- [24] L. Wang, S. Fortunati, M. S. Greco, and F. Gini, "Reinforcement learning-based waveform optimization for MIMO multi-target detection," in *2018 52nd Asilomar Conference on Signals, Systems, and Computers*, Oct 2018, pp. 1329–1333.
- [25] L. Wang, Y. Zhang, Q. Liao, and J. Tang, "Robust waveform design for multi-target detection in cognitive MIMO radar," in *2018 IEEE Radar Conference (RadarConf18)*, April 2018, pp. 0116–0120.
- [26] B. Friedlander, "On transmit beamforming for MIMO radar," *IEEE Transactions on Aerospace and Electronic Systems*, vol. 48, no. 4, pp. 3376–3388, October 2012.
- [27] K. J. Sangston and K. R. Gerlach, "Coherent detection of radar targets in a non-Gaussian background," *IEEE Transactions on Aerospace and Electronic Systems*, vol. 30, no. 2, pp. 330–340, April 1994.
- [28] S. Fortunati, F. Gini, M. S. Greco, and C. D. Richmond, "Performance bounds for parameter estimation under misspecified models: Fundamental findings and applications," *IEEE Signal Processing Magazine*, vol. 34, no. 6, pp. 142–157, Nov 2017.
- [29] K. J. Sangston, F. Gini, and M. Greco, "Coherent radar target detection in heavy-tailed compound-Gaussian Clutter," *IEEE Transactions on Aerospace and Electronic Systems*, vol. 48, pp. 64–77, 2012.
- [30] M. Mohri, A. Rostamizadeh, and A. Talwalkar, *Foundations of Machine Learning*. The MIT Press, 2012.
- [31] A. H. Nuttall, "Some integrals involving the (q sub m)-function," 1974.
- [32] D. Poole and A. Mackworth, *Artificial Intelligence: Foundations of Computational Agents*, 2nd ed. Cambridge, UK: Cambridge University Press, 2017. [Online]. Available: <http://artint.info/2e/html/ArtInt2e.html>
- [33] Z. Luo, W. Ma, A. M. So, Y. Ye, and S. Zhang, "Semidefinite relaxation of quadratic optimization problems," *IEEE Signal Processing Magazine*, vol. 27, no. 3, pp. 20–34, 2010.
- [34] J. Lipor, S. Ahmed, and M.-S. Alouini, "Fourier-based transmit beam-pattern design using MIMO radar," *IEEE Transactions on Signal Processing*, vol. 62, pp. 2226–2235, 2014.
- [35] D. R. Fuhrmann and G. San Antonio, "Transmit beamforming for MIMO radar systems using signal cross-correlation," *IEEE Transactions on Aerospace and Electronic Systems*, vol. 44, no. 1, pp. 171–186, 2008.
- [36] G. Scutari, F. Facchini, L. Lampariello, P. Song, and S. Sardellitti, "Parallel and distributed methods for nonconvex optimization-part II: applications," *CoRR*, vol. abs/1601.04059, 2016. [Online]. Available: <http://arXiv.org/abs/1601.04059>
- [37] M. Grant and S. Boyd, "CVX: Matlab software for disciplined convex programming, version 2.1," <http://cvxr.com/cvx>, Mar. 2014.
- [38] S. Fortunati, F. Gini, and M. S. Greco, "The misspecified Cramer-Rao bound and its application to scatter matrix estimation in complex elliptically symmetric distributions," *IEEE Transactions on Signal Processing*, vol. 64, no. 9, pp. 2387–2399, 2016.
- [39] H. White and I. Domowitz, "Nonlinear regression with dependent observations," *Econometrica*, vol. 52, no. 1, pp. 143–161, 1984. [Online]. Available: <http://www.jstor.org/stable/1911465>